Modelling and analysis of nucleon emission from deuteron-induced reactions at incident energies up to 100 MeV

Shinsuke Nakayama[1a], Hiroshi Kouno[2], Yukinobu Watanabe[2], Osamu Iwamoto[1], Tao Ye[3], and Kazuyuki Ogata[4]

[1]*Nuclear Science and Engineering Center, Japan Atomic Energy Agency, 2-4, Shirakata, Tokai-mura, Ibaraki, 319-1195, Japan*
[2]*Department of Advanced Energy Engineering Science, Kyushu University, 6-1, Kasuga-koen, Kasuga-shi, Fukuoka 816-8580, Japan*
[3]*Institute of Applied Physics and Computational Mathematics, Beijing, 100094, China*
[4]*Research Center for Nuclear Physics, Osaka University, 10-1, Mihogaoka, Ibaraki-shi, Osaka, 567-0047, Japan*

Abstract. We have so far developed a computational code system dedicated to deuteron-induced reactions in combination with some theoretical models. In our previous works, the code system was successfully applied to systematic analyses of double-differential cross sections (DDXs) of (*d*,*xp*) reactions for ^{12}C, ^{27}Al, and ^{58}Ni at incident energies up to 100 MeV. In the present work, we apply the code system to neutron emission from deuteron-induced reactions. Since there is few experimental data of DDXs of (*d*,*xn*) reactions, double-differential thick target neutron yields (TTNYs) are calculated and compared with experimental data instead of DDXs. The calculation using the code system reproduces the measured TTNYs for carbon at incident energies up to 50 MeV.

1 Introduction

In recent years, research and development of accelerator neutron sources has led to renewed interest in the study of deuteron-induced reactions. In these facilities, the (*d*,*xn*) reaction on light nuclei (Li, Be, C, etc.) is considered as a promising reaction to generate intensive neutron beams. Fig.1 shows experimental thick target neutron yields (TTNYs) from (*p*,*xn*) and (*d*,*xn*) reactions on ^{9}Be [1, 2]. This figure shows some advantages of a (*d*,*xn*) neutron source over a widely-used (*p*,*xn*) neutron source. First, the amount of generated neutrons is large. Second, the neutron spectrum has a broad energy peak around half the deuteron incident energy. This means that the most probable neutron energy can be changed by adjusting incident deuteron energy. In addition, the (*d*,*xn*) reaction has strongly forward-peaked angular distribution, which is an additional advantage from the point of view of shielding. From these favourable features, intensive neutron sources using deuteron accelerator have been proposed for various applications such as production of radioisotopes for medical use [3, 4] and irradiation testing of fusion reactor materials [5].

Engineering design of such (*d*,*xn*) neutron sources requires understanding of the interaction of deuteron with various materials used in the system components, e.g., a neutron converter, a beam collimator, a vacuum duct, etc. Therefore, we have so far developed a computational code system

[a] Corresponding author: nakayama.shinsuke@jaea.go.jp

dedicated to deuteron-induced reactions in combination with some theoretical models [6-9]. Elastic breakup and stripping reactions to continuum are calculated using the codes based on the Continuum-Discretized Coupled-Channels method (CDCC) [10] and the Glauber model [6], respectively. In addition, DWUCK4 [11], which is the calculation code based on conventional zero-range Distorted Wave Born Approximation (DWBA), is used to calculate stripping reactions to bound states in the residual nuclei. Finally, preequilibrium and evaporation components are estimated using the CCONE code [12], which was successfully applied to neutron nuclear data evaluation for the latest version of Japanese Evaluated Nuclear Data Library (JENDL-4.0) [13]. In our previous works, the code system has been successfully applied to systematic analyses of double-differential cross sections (DDXs) of (*d*,*xp*) reactions for ^{12}C, ^{27}Al, and ^{58}Ni at incident energies up to 100 MeV [7-9]. The calculation is in good agreement with the experimental data. This result shows that the neutron stripping process to continuum is dominant in forward proton emission in the high incident energy region.

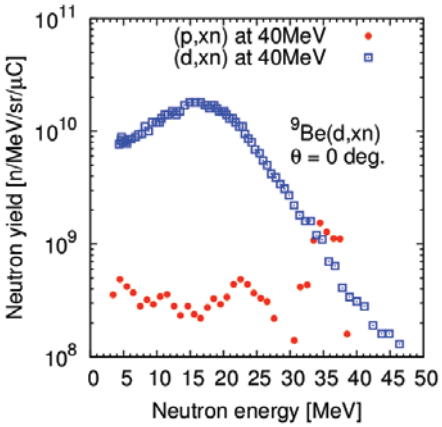

Figure 1. Experimental double defferential thick target neutron yields from (*p*,*xn*) and (*d*,*xn*) reactions on ^{9}Be at 40 MeV. The data are taken from Refs. [1,2].

In this study, we apply the code system to neutron emission from deuteron-induced reactions. Since there is few experimental data of DDXs of (*d*,*xn*) reactions, TTNYs for carbon are calculated and compared with the corresponding experimental data instead of DDXs. The measured TTNYs for carbon are available in the wide incident energy range, thus they enable us to investigate the incident energy dependence of individual reaction processes in detail. Including the results of our previous works for the (*d*,*xp*) reactions, validation of the present modelling for both proton and neutron emissions from deuteron-induced reactions is discussed through comparison with available experimental data.

2 Analysis of stripping reactions by DWBA

First of all, we analyze the stripping reaction process to discrete states by DWBA. These reactions make a large contribution to nucleon emission in the low incident energy region. In TTNYs calculation, we assume that natural carbon consists of only ^{12}C isotope whose natural abundance is 98.89%. Therefore, we analyze the ^{12}C(*d*,*n*)^{13}N reactions to the ground and some excited states.

2.1 DWBA calculation

The DWBA differential cross section for the (*d*,*n*) reaction leading to the bound state *i* is given by

$$\frac{d\sigma_{DWBA,i}}{d\Omega}(E_d) = \frac{D_0^2}{10^4}\frac{2J_i+1}{2J_A+1}\frac{S_i}{2j+1}\frac{d\sigma_{DWUCK4,i}}{d\Omega}(E_d) \quad (1)$$

where E_d is the incident deuteron energy, D_0 is a constant used in zero-range approximation, J_A and J_i are the spins of target nucleus ^{12}C and i-th state of residual nucleus ^{13}N, respectively, S_i is the spectroscopic factor for each state, j is the spin of transferred proton, and $d\sigma_{DWUCK4,i}/d\Omega$ is the differential cross section calculated with the DWUCK4 code. Input parameters used in DWUCK4 calculations are listed in Table 1. These parameters are based on our previous work [9].

Table 1. Input parameters used in the DWUCK4.

Neutron potential	Koning-Deraloche (KD) [14]
Deuteron potential	Adiabatic potential [15] from KD
Proton binding potential	Woods-Saxon form r_0 = 1.25 (fm), a_0 = 0.65 (fm)
Finite range correction factor (fm)	0.7457
Zero range constant D_0^2 (MeV^{2}fm^3)	1.5×10^4
Nonlocality parameters	neutron:0.85, deuteron:0.54

In the DWBA analyses for the ^{12}C(d,n)^{13}N reactions, we consider the four states of ^{13}N where experimental differential cross sections are available [16-20], namely the ground state (J^π=1/2$^-$), the first excited state (E_x= 2.37 MeV, J^π= 1/2$^+$), the second excited state (E_x= 3.51 MeV, J^π= 3/2$^-$), and the third excited state (E_x= 3.55 MeV, J^π= 5/2$^+$). The excited states of ^{13}N are unbound since the proton separation energy of ^{13}N is 1.94MeV. Following Ref. [18], we have calculated the DWBA cross section for these state using a very loosely bound state wave function by setting the binding energy to 0.01MeV in DWUCK4 calculations. In addition, the statistical decay contribution from compound nuclei is calculated using the CCONE code.

Figure 2 shows the comparison of calculated and experimental differential cross sections for the ^{12}C(d,n)^{13}N reactions in the incident energy range from 7 to 18 MeV. The experimental data are taken from Refs. [16–20]. The values of spectroscopic factor (SF) are extracted by fitting the calculated DWBA cross section to the corresponding experimental one at forward angles where proton stripping process is dominant. It should be noted that the experimental values for the second and the third excited states are unresolved. From the analyses for the ^{12}C(d,p)^{13}C, which is the isobaric analog state of ^{13}N [9], we estimate the SF values of the third excited state which is four times as large as that of the second excited state. The sum of the direct stripping component calculated by DWBA and the contribution from statistical decay show good agreement with the experimental data at small angles.

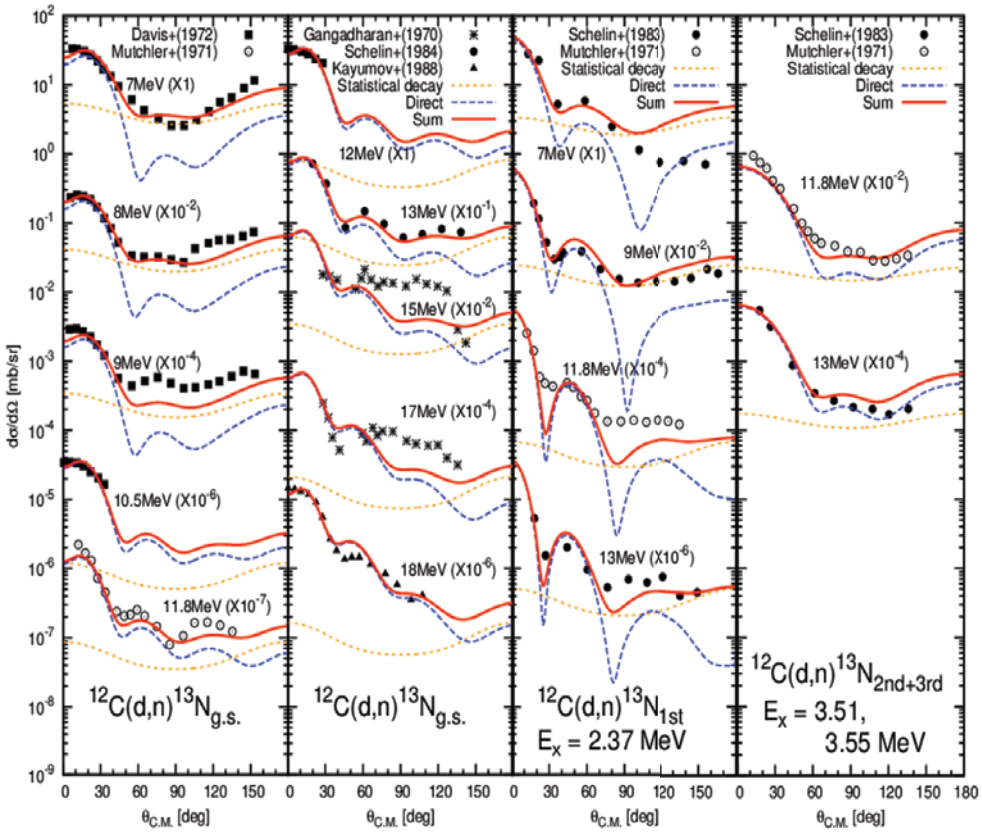

Figure 2. Calculated and experimental differential cross sections for the $^{12}C(d,n)^{13}N$ reaction.

2.2 Spectroscopic factor

The experimental SF values for the $^{12}C(d,n)^{13}N$ reaction extracted from the present analyses are shown in Table 2. They are also presented in solid squares in Fig.3. Fluctuation among the experimental SF values can be seen in the figure. This is due to the effect of resonance structures as described in Ref. [16].

Table 2. List of spectroscopic factors for the $^{12}C(d,n)^{13}N$ reaction extracted from the present analysis

i	E_x (MeV)	J^π	l	$S_i(E_d)$									
				7	8	9	10.5	11.8	12	13	15	17	18
0	0 (g.s.)	$\frac{1}{2}^-$	1	0.50	0.46	0.42	0.93	0.40	1.00	0.28	0.30	0.31	0.69
1	2.37	$\frac{1}{2}^+$	0	0.29	-	0.43	-	0.54	-	0.39	-	-	-
2	3.51	$\frac{3}{2}^-$	1	-	-	-	-	0.66	-	0.64	-	-	-
3	3.55	$\frac{5}{2}^+$	2	-	-	-	-	0.17	-	0.16	-	-	-

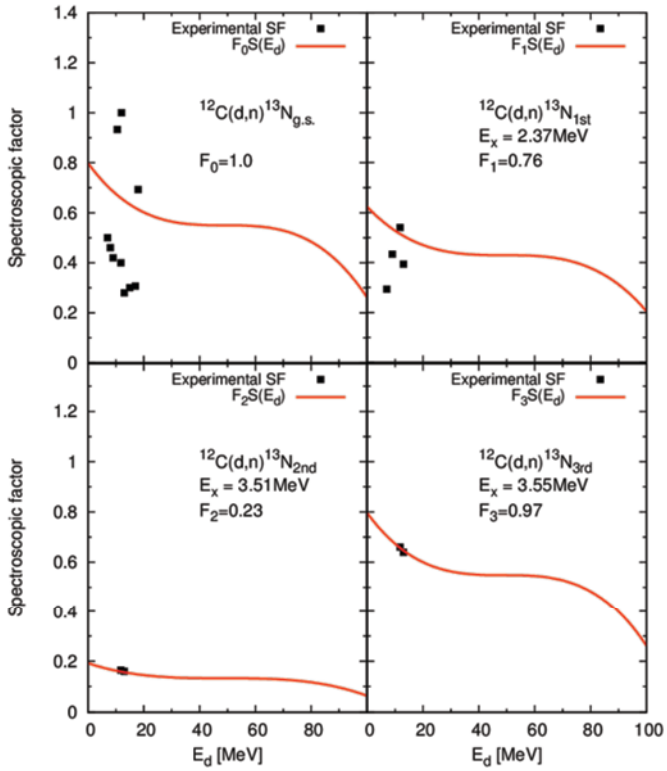

Figure 3. Experimental and empirical spectroscopic factors for the ^{12}C(d,n)^{13}N reaction.

In our systematic DWBA analyses for the (d,p) reactions on ^{12}C, ^{27}Al, ^{40}Ca, and ^{58}Ni, the extracted SF values have shown similar incident energy dependence for all the target nuclei. Therefore, we proposed the following empirical expression to express the energy dependence of the experimental SF values [9] :

$$S(E_d) = -2.18\times10^{-6}E_d^3 + 3.19\times10^{-4}E_d^2 - 1.56\times10^{-2}E_d + 8.20\times10^{-1}. \quad (2)$$

We assume that the SF value for each ^{12}C(d,n)^{13}N reaction has the same energy dependence as $S(E_d)$. Since $S(E_d)$ is re-normalized for the case of the ^{12}C(d,p)^{13}C$_{g.s.}$ reaction, it is necessary to fix a scaling factor F_i depending on each i-th state of ^{13}N. We average the effect of resonance structures and fix the each F_i as follows. For the ground and the first excited states of ^{13}N, we adopt the same F_i as the ones for the corresponding states of ^{13}C derived in Ref. [9]. For the second and the third excited state of ^{13}N, we fix each F_i so as that $F_iS(E_d)$ pass through the center of experimental SF values. The empirical SF values $F_iS(E_d)$ for the each reaction are shown by solid line in Fig. 3.

3 Analysis of TTNYs

In the engineering design of deuteron accelerator neutron sources, DDXs for (d,xn) reactions are critically important. However, the experimental data are sparse over wide ranges of target mass number and incident energy. On the other hand, experimental data of TTNYs for carbon are available in the wide incident energy range. To validate the present modelling for neutron emission from deuteron-induced reactions, we derive TTNYs from DDXs for (d,xn) reactions calculated with the present code system and compare the resultant TTNYs with the experimental data.

3.1 Calculation method

In TTNYs calculation, we assume that natural carbon consists of only ^{12}C. TTNYs for the ^{12}C target can be derived as

$$\frac{d^2Y}{dEd\Omega}(E_d) = N\int_0^{E_d} dE_i \frac{d^2\sigma}{dEd\Omega}(E_i)\left[\frac{dE_i}{dx}\right]^{-1} \exp\left(-N\int_{E_i}^{E_d} dE'\sigma_{rea}(E')\left[\frac{dE'}{dx}\right]^{-1}\right) \quad (3)$$

where E_d is the incident deuteron energy, N is the atomic density of the target, E_i is the deuteron energy in the target, $d^2\sigma/dEd\Omega$ is the DDXs for the ^{12}C(d,xn) reaction, dE/dx is the deuteron stopping power of deuteron in the ^{12}C target, and σ_{rea} is the deuteron total reaction cross section on ^{12}C.

We calculate the stopping power and the total reaction cross section with the SRIM-2010 code [21] and the CCONE code, respectively. DDXs for the ^{12}C(d,xn) reaction are calculated in the same way as described in Refs. [8, 9].The input parameters in DWBA calculations are the same as those given in Table 1. In the CDCC and Glauber models, nucleon optical potentials (OPs) of KD [14] are used for proton and neutron. The OPs used in the CCONE code are the global nucleon OPs of KD for proton and neutron and the adiabatic OP [15] for deuteron in a consistent way as in DWBA calculations. Default values in the CCONE code are used for other input parameters such as the level density parameter. The SF values for the ^{12}C(d,n)^{13}N reactions are given by each $F_iS(E_d)$ shown in Fig. 2.

3.2 Results and discussion

Figure 4 shows the comparisons between the calculated and experimental TTNYs for carbon at angles around 0°. The incident deuteron energies are from 9 to 50 MeV. The experimental data are taken from Refs. [22-27].

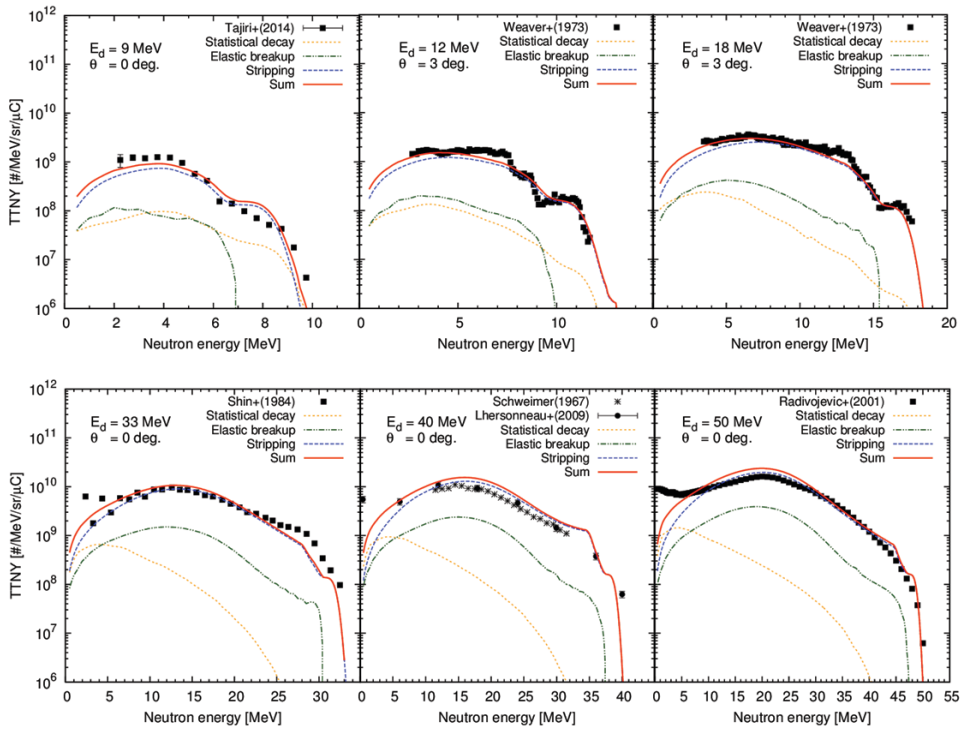

Figure 4. Calculated and experimental TTNYs for carbon in the incident energy from 9 to 50 MeV.

In the wide incident energy range, the present calculation reproduces both the shape and magnitude of the experimental TTNY spectra at forward angles around 0°. As shown in Fig.4, the proton stripping process is dominant in the incident energy below 50 MeV. In our previous works [6-9], the calculation results have shown that the neutron stripping process is dominant in forward proton emission at 56 and 100 MeV. These results indicate that the stripping processes make a dominat contribution to neucleon emission in the whole incident energy range below 100 MeV and they should be taken into account using reliable theoretical models. However, the present calculation fails to reproduce the TTNY spectra in the low emission energy region. This discrepancy may be due to insufficiency of the statistical decay calculation.

Figure 5 shows the comparisons between the calculated and experimental TTNYs for carbon for several angles at 18 MeV. The present calculation reproduces the experimental data at several forward angles. It should be noted that the step structure seen in the high energy region arises from the stripping reaction to the ground and some excited states of ^{13}N calculated by DWBA. The Glauber model cannot deal with individual transitions to bound states but can describe the sum of stripping contributions to both continuum and bound states as a continuous spectrum. Thus, if we use the Glauber model alone to calculate the stripping component, these step structure in TTNYs cannot be reproduced well.

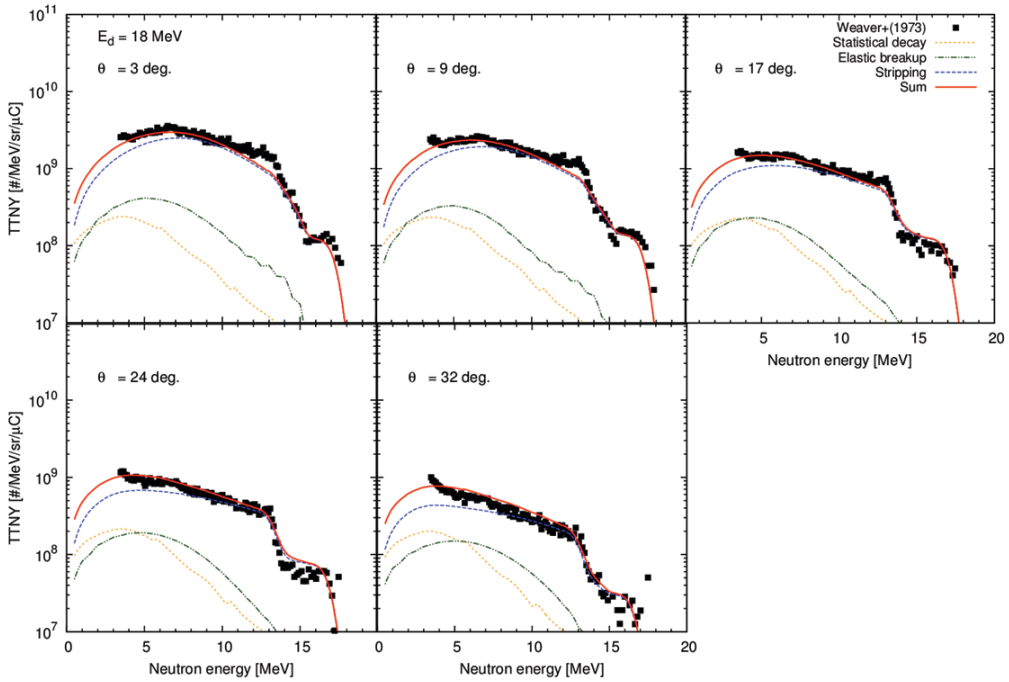

Figure 5. Calculated and experimental TTNYs for carbon at 18 MeV.

4 Summary and outlook

A computational code system dedicated to deuteron-induced reactions has been applied to neutron emission in deuteron-induced reactions. The code system consists of the codes based on the CDCC for elastic breakup and the Glauber model for the stripping reaction to continuum, DWUCK4 based on conventional zero-range DWBA for the stripping reaction to bound states in the residual nuclei, and the CCONE code for preequilibrium and evaporation components. The calculations with the code system reproduce successfully the experimental thick target neutron yields (TTNYs) for carbon at incident energies from 9 to 50 MeV. Along with the results of our previous works for double

differential (*d*,*xp*) cross sections, these results demonstrate the applicability of the present modelling for both proton and neutron emissions from deuteron-induced reactions.

In the future, we plan to apply the present modelling to analyses of TTNYs for other nuclei, such as Be, Li, Al, etc., which are required in the engineering design of deuteron accelerator neutron sources.

Acknowledgement

The authors wish to thank S. Hashimoto for fruitful discussion and comments on DWBA analyses.

References

1. M.J. Saltmarsh, C.A. Ludemann, C.B. Fulmer, R.C. Styles, Nucl. Instr. Meth. **145**, 81-90 (1977).
2. Y. Uwamino, T. Okubo, A. Torii, T. Nakamura, Nucl. Instrum. Methods Phys. Res. A **271**, 546 (1988).
3. Y. Nagai, K. Hashimoto, Y. Hatsukawa, H. Saeki, S. Motoishi, N. Sato, M. Kawabata, H. Harada, T. Kin, K. Tsukada, T. Sato, F. Minato, O. Iwamoto, N. Iwamoto, Y. Seki, K. Yokoyama, T. Shiina, A. Ohta, N. Takeuchi, Y. Kawauchi, N. Sato, H. Yamabayashi, Y. Adachi, Y. Kikuchi, T. Mitsumoto, T. Igarashi, J. Phys. Soc. Jpn. **82**, 064201 (2013).
4. T. Kin, Y. Nagai, N. Iwamoto, F. Minato, O. Iwamoto, Y. Hatsukawa, M. Segawa, H. Harada, C. Konno, K. Ochiai, K. Takakura, J. Phys. Soc. Jpn. **82**, 034201 (2013).
5. A. Moeslang, V. Heinzel, H. Matsui, M. Sugimoto, Fusion Eng. Des. **81**, 863 (2006).
6. T. Ye, S. Hashimoto, Y. Watanabe, K. Ogata, M. Yahiro, Phys. Rev. C **84**, 054606 (2011).
7. S. Nakayama, S. Araki, Y. Watanabe, O. Iwamoto, T. Ye, K. Ogata, Nucl. Data Sheets **118**, 305 (2014).
8. S. Nakayama, S. Araki, Y. Watanabe, O. Iwamoto, T. Ye, K. Ogata, Energy Procedia **71**, 219 (2015).
9. S. Nakayama, Y. Watanabe, J. Nucl. Sci. Technol. (2015) *in press*.
10. M. Yahiro, K. Ogata, T. Matsumoto, K. Minomo, Prog. Theor. Exp. Phys. **2012**, 01A206 (2012) and references therein.
11. P.D. Kunz, computer code DWUCK4 (1974), http://spot.colorado.edu/~kunz/DWBA.html.
12. O. Iwamoto, J. Nucl. Sci. Technol. **44**, 687 (2007).
13. K. Shibata, O. Iwamoto, T. Nakagawa, N. Iwamoto, A. Ichihara, S. Kunieda, S. Chiba, K. Furutaka, N. Otuka, T. Ohsawa, T. Murata, H. Matsunobu, A. Zukeran, S. Kamada, J. Katakura, J. Nucl. Sci. Technol. **48**, 1 (2011).
14. A.J. Koning, J.P. Delaroche, Nucl. Phys. A **713**, 231 (2003).
15. D.G. Madland, Proc. Specialists' Meeting on Preequilibrium Nuclear Reactions, 103, Semmering, Austria, 10-12 Feb (1988).
16. J.R. Davis, G. U. Din, Nucl. Phys. A **179**, 101 (1972).
17. H.R. Schelin, E. Farrelly Pessoa, W.R. Wylie, E.W. Cybulska, K. Nakayama, L.M. Fagundes, R.A. Douglas, Nucl. Phys. A **414**, 67 (1984).
18. G.S. Matchler, D. Rendic, D.E. Velkley, W.E. Sweeney jr., G.C. Phillips, Nucl. Phys. A **172**, 469 (1971).
19. S. Gangadharan, R.L. Wolke, Phys. Rev. C **1**, 1333 (1970).
20. M.A. Kayumov, S.S. Kayumov, S.P. Krekoten, A.M. Mukhamedzhanov, K.D. Razikov, K. Khamidova, R. Yarmukhamedov, Sov. J. Nucl. Phys. **48**, 629 (1988).
21. J. F. Ziegler, M. D. Ziegler, and J. P. Biersack, Nucl. Instrum. Methods Phys. Res. B **268**, 1818 (2010).
22. Y. Tajiri, Y. Watanabe, N. Shigyo, K. Hirabayashi, T. Nishizawa, K. Sagara, Prog. Nucl. Sci. Technol. **4**, 582 (2014).
23. K.A. Weaver, J.D. Anderson, H.H. Barschall, J.C. Davis, Nucl. Sci. Eng. **52**, 35 (1973).

24. K. Shin, K. Hibi, M. Fujii, Y. Uwamino, T. Nakamura, Phys. Rev. C **29**, 1307 (1984).
25. G. Lhersonneau, T. Malkiewicz, K. Kolos, M. Fadila, H. Kettunen, M.G. Saint-Laurent, A. Pichard, W.H. Trzaska, G. Tyurin, L. Cousin, Nucl. Instrum. Methods Phys. Res. A **603**, 228 (2009).
26. G.W. Schweimer, Nucl. Phys. A **100**, 537 (1967).
27. Z. Radivojevic, A. Andrighetto, F. Brandolini, P. Dendooven, A. Honkanen, J. Aysto, V. Lyapin, V. Rubchenya, W.H. Trzaska, D. Vakhtin, G. Walter, Nucl. Instrum. Methods Phys. Res. B **183**, 212 (2001).